Journal of Engineering Mathematics **36:** 207–218, 1999.

The local flow in a wedge between a rigid wall and a surface of constant shear stress

HENDRIK C. KUHLMANN, CHRISTIAN NIENHÜSER and HANS J. RATH
ZARM - Universität Bremen, 28359 Bremen, Germany; e-mail: kuhl@zarm.uni-bremen.de

Received 9 April 1998; accepted in revised form 4 December 1998

Abstract. The viscous incompressible flow in a wedge between a rigid plane and a surface of constant shear stress is calculated by use of the Mellin transform. For wedge angles below a critical value the asymptotic solution near the vertex is given by a local similarity solution. The respective stream function grows quadratically with the distance from the origin. For supercritical wedge angles the similarity solution breaks down and the leading order solution for the stream function grows with a power law having an exponent less than two. At the critical angle logarithmic terms appear in the stream function. The asymptotic dependence of the stream function found here is the same as for the 'hinged plate' problem. It is shown that the validity of the Stokes flow assumption is restricted to a vanishingly small distance from the vertex when the wedge angle is above critical and when the region of nonzero constant shear stress is extended to infinity. The relevance of the present result for technical flow systems is pointed out by comparison with the numerically calculated flow in a thermocapillary liquid bridge.

Key words: thermocapillary flow, corner flow, Mellin transform, singularity.

1. Introduction

Fluid flow in wedges is a fundamental problem in fluid mechanics. It can be traced back to Taylor [1, 2] who considered the scraping of a viscous fluid from a plane surface. Moffatt [3] extended the analysis to incompressible flows in infinite wedges satisfying different sets of boundary conditions. He derived simple similarity solutions for a number of Stokes flow wedge problems. While for some problems like, *e.g.*, the flow in a rigid corner the local similarity solution is valid for all wedge angles α, the similarity solution breaks down, i.e. the stream function diverges, for other wedge flow problems when the wedge angle approaches a critical value. Among these latter problems are the pressure driven flow along a cylindrical tube whose cross-section has a sharp corner, or the 'hinged plate' problem. Both configurations have been treated by Moffatt and Duffy [4].

Stokes flow in corners has also been studied by other authors. Recently, Anderson and Davis [5] considered viscous flow in a wedge made up by one rigid and one stress-free boundary. Moreover, local solutions and partially local solutions, the latter ones do not satisfy all boundary conditions, were calculated for a rigid wedge where two immiscible viscous fluids meet at the vertex. In a later paper the same authors investigated the flow near a tri-junction including heat transfer and solidification [6]. Other boundary conditions have been considered by Betelú *et al.* [7]. Neglecting surface tension they calculated the viscous flow and its temporal evolution in a corner bounded by two stress-free surfaces initially forming a sharp wedge. Neither of these studies, however, was devoted to the case when one wall is subject to a given nonzero tangential stress.

Here, we consider a problem similar to that of [4] which is motivated by the flow in crystal growth melts. In the floating zone method [8], for instance, a melt volume is suspended between two cylindrical solid rods of the same material, the temperature of which is close to the melting point. The molten material forms a liquid bridge which is kept in place solely by surface tension forces which are very high for liquid metals. Owing to the thermal conditions near the contact point where liquid, solid, and ambient gas meet, the temperature drops from the contact point and along the liquid/gas interface. The associated temperature gradients can drive a significant fluid motion via the thermocapillary effect. The flow structure near the contact point (contact line in three dimensions) is of particular importance for numerical simulations, since a number of difficulties are encountered in that region.

First, the contact line represents a discontinuity of the boundary conditions which, in the presence of even weak thermocapillary flow, leads to pressure peaks in the corner that can only be balanced by surface tension. The situation is similar to that in the die-swell problem (see, *e.g.* [9]). As a consequence, the curvature of the interface must become infinitely large at the contact point. This problem is not present in the limit of infinitely large mean surface tension, where the meniscus shape is determined independently of the flow field, and the corner region may be modelled by a wedge made of a rigid isothermal plane wall and a thermocapillary surface. To first order the temperature will vary linearly from the contact line and thus the thermocapillary shear stress will be constant in a small neighborhood of that line.

The associated problem of creeping flow in an infinite wedge has a similarity solution $\psi \sim r^2$, where ψ is the stream function and r the distance from the vertex [10]. The second problem is that the similarity solution breaks down for $\alpha = \alpha_c$ [11, p. 323] and predicts a flow reversal for $\alpha > \alpha_c$. This counter-intuitive behavior of the Stokes flow solution motivated Shevtsova *et al.* [11] to numerically investigate the full nonlinear Navier-Stokes flow near the corner. By successive subdivisions of the integration area for $\alpha = 135^\circ > \alpha_c$ they did not find, however, any flow reversal neither near the cold nor near the hot corner.

To resolve the latter problem we shall look for solutions that are not of self-similar type and inquire about their asymptotic form for $r \to 0$. The analysis follows closely that of Moffatt [12] and Moffatt and Duffy [4]. The idea is the following. We transform the stream function $\psi(r, \theta)$ of the real radial coordinate r into a stream function $\bar{\psi}(p, \theta)$ for a complex coordinate p. Since this is achieved by an integral transform, the radial derivatives can be eliminated from the differential equation by integrations by parts. We will be left with an ordinary differential equation in θ which can be solved analytically. The solution is then transformed back into physical space. The back-transformation involves a line integral in the complex p-plane which can be closed at infinity and the solution can be expressed as a sum over the residues of $\bar{\psi}$. The residue of the pole with the smallest real part determines the asymtotic behavior for $r \to 0$.

The paper is organized as follows. First, we define the problem in Section 2 and present the similarity solution in Section 3. The problem is then solved by use of the Mellin transform in Section 4. In Section 5 we consider the asymptotic form of the solution for $r \to 0$ and close in Section 6 with a discussion of the results and a comparison with a full numerical solution near the contact point.

2. Formulation of the problem

We consider the two-dimensional flow in a corner made by a rigid plane enclosing an angle α with a flat surface along which a constant shear stress is exerted on the liquid (cf. Figure 1).

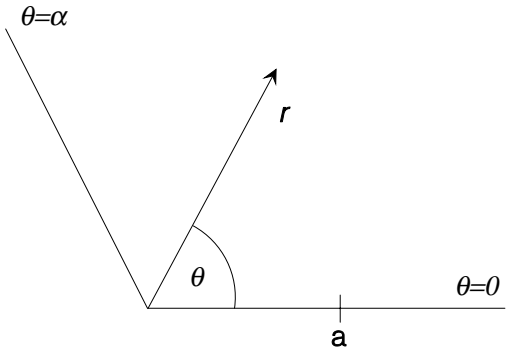

Figure 1. Geometry of the problem.

It is assumed that the flow close to the vertex is slow and that it is governed by the Stokes equation

$$\nabla^4 \psi(r, \theta) = 0, \tag{1}$$

for the stream function ψ, defined by

$$u = \frac{1}{r}\partial_\theta \psi, \qquad v = -\partial_r \psi, \tag{2}$$

where r and θ are polar coordinates and u and v the radial and azimuthal velocity, respectively. The no-slip and no-penetration boundary conditions along the rigid wall at $\theta = \alpha$ and the constant shear stress ω_0 and no-penetration conditions along the liquid/gas interface at $\theta = 0$ are

$$\begin{aligned} &\theta = 0: \qquad \partial_r \psi = 0, \qquad \partial_\theta^2 \psi = \begin{cases} \omega_0 r^2, & r \leqslant a, \\ 0, & r > a, \end{cases} \\ &\theta = \alpha: \qquad \partial_r \psi = 0, \qquad \partial_\theta \psi = 0, \end{aligned} \tag{3}$$

where ω_0 is a positive constant. These boundary conditions are to model the real conditions near a cold thermocapillary corner. Owing to the method of solution the region of constant shear stress is limited here to a finite length a beyond which the surface is assumed stress-free.

3. Similarity solution

The problem (1, 3) with $a \to \infty$ admits a scale-independent local similarity solution

$$\psi = \omega_0 r^2 f(\theta), \tag{4}$$

where f must satisfy

$$(\partial_\theta^4 + 4\partial_\theta^2) f(\theta) = 0, \tag{5}$$

subject to the boundary conditions

$$f(\alpha) = f'(\alpha) = f(0) = f''(0) - 1 = 0. \tag{6}$$

The solution is

$$f(\theta) = A\ \cos\ 2\theta + B\ \sin\ 2\theta + C\theta + D, \tag{7}$$

with the four integration constants

$$A = -\frac{1}{4}, \qquad B = \frac{1}{4}\,\frac{\cos\ 2\alpha + 2\alpha\ \sin\ 2\alpha - 1}{\sin\ 2\alpha - 2\alpha\ \cos\ 2\alpha},$$

$$C = \frac{1}{2}\,\frac{\cos\ 2\alpha - 1}{\sin\ 2\alpha - 2\alpha\ \cos\ 2\alpha}, \quad D = \frac{1}{4}, \tag{8}$$

determined by (6). This solution has also been given by Canright [10]. The vorticity $\omega = -4\omega_0(C\theta + D)$ depends only on the angle θ. Therefore, the solution is singular at the origin $r = 0$. The solution becomes singular everywhere in the volume when

$$\sin\ 2\alpha - 2\alpha\ \cos\ 2\alpha = 0. \tag{9}$$

The only nontrivial root in the interval $[0, \pi]$ is $\alpha_c = 0{\cdot}715\ \pi = 2{\cdot}2467 = 128{\cdot}7°$. At this contact angle, the plane on which the vorticity vanishes coincides with the free surface. The boundary conditions (3), however, impose a constant nonzero vorticity $\omega = -\omega_0$ on the free surface. Therefore, the vorticity field must exhibit strong gradients all along the free surface when $\alpha \approx \alpha_c$. As a result high velocity gradients arise and the streamlines become asymptotically dense for $\alpha \to \alpha_c$. For $\alpha < \alpha_c$ and $\omega_0 > 0$ the flow on the free surface is directed towards the corner ($u(\theta = 0) < 0$), while the similarity solution predicts a flow away from it ($u(\theta = 0) > 0$) for $\alpha > \alpha_c$. Since the solution breaks down at $\alpha = \alpha_c$, the question arises, whether the similarity solution is a local solution of (1,3) for $\alpha > \alpha_c$. To answer this question, we solve the problem without the assumption of separability.

4. General solution

We seek a the solution of (1, 3) using the Mellin transformation in a way described by Tranter [13]. The Mellin transform is given by

$$\bar{\psi}(p, \theta) = \int_0^\infty r^{p-1}\psi(r, \theta)\,\mathrm{d}r, \tag{10}$$

while the back-transformation is

$$\psi(r, \theta) = \frac{1}{2\pi\ \mathrm{i}}\int_{c-\mathrm{i}\infty}^{c+\mathrm{i}\infty} r^{-p}\bar{\psi}(p, \theta)\,\mathrm{d}p, \tag{11}$$

where $p \in \mathbb{C}$ and $c \in \mathbb{R}$. As we shall see later on, we will have to use $\Re(p) = -1$. Therefore, the transform $\bar{\psi}$ exists, if ψ satisfies the asymptotic relations

$$\psi(r, \theta) = \begin{cases} O(r^{1+\varepsilon}), & r \to 0, \\ O(r^{1-\varepsilon}), & r \to \infty, \end{cases} \tag{12}$$

which must be checked *a posteriori*.

Multiplying (1) by r^{p+3} and integrating from 0 to ∞ we obtain the transformed biharmonic equation

$$[\partial_\theta^4 + ((p+2)^2 + p^2)\partial_\theta^2 + p^2(p+2)^2]\bar{\psi} = 0, \tag{13}$$

where we have used that the boundary terms vanish, since they are $o(r^\varepsilon)$ for $r \to 0$ and $o(r^{-\varepsilon})$ for $r \to \infty$, respectively. Similarly, one obtains the transformed boundary conditions

$$\begin{aligned} &\theta = 0: \qquad \bar{\psi} = 0, \qquad \partial_\theta^2 \bar{\psi} = \omega_0 \int_0^a r^{p-1} r^2 \,\mathrm{d}r = \omega_0 \frac{a^{p+2}}{p+2}, \\ &\theta = \alpha: \qquad \bar{\psi} = 0, \qquad \partial_\theta \bar{\psi} = 0. \end{aligned} \tag{14}$$

The solution of (13) has the form

$$\bar{\psi} = A\,\mathrm{e}^{\mathrm{i}p\theta} + B\,\mathrm{e}^{-\mathrm{i}p\theta} + C\,\mathrm{e}^{\mathrm{i}(p+2)\theta} + D\,\mathrm{e}^{-\mathrm{i}(p+2)\theta}. \tag{15}$$

Inserting this into the boundary conditions, we obtain the unique solution

$$\bar{\psi}(p,\theta) = \frac{\omega_0 a^{p+2}}{4} \frac{F(\theta, p)}{W(p)(p+1)(p+2)}, \tag{16}$$

with

$$\begin{aligned} F(\theta, p) \;=\; & (p+1)\sin[(p+2)\theta - 2\alpha] \\ & - \sin[(p+2)\theta - 2(p+1)\alpha] - p\,\sin[(p+2)\theta] \\ & -(p+2)\sin[p\theta] + (p+1)\sin[p\theta + 2\alpha] + \sin[p\theta - 2(p+1)\alpha], \end{aligned} \tag{17}$$

and

$$W(p) = (p+1)\,\sin[2\alpha] - \sin[2(p+1)\alpha]. \tag{18}$$

Since we shall have to integrate $\bar{\psi}$ along $\Re(p) = -1$, it is important to note that $\bar{\psi}$ has a removable singularity at $p = -1$ (the denominator has a double zero, and $F = F' = 0$).

For later use we now establish a symmetry which relates $\bar{\psi}(-p)$ to $\bar{\psi}(p-2)$. It is readily confirmed that

$$F(\theta, -p) = F(\theta, p-2), \tag{19}$$

$$W(-p) = -W(p-2). \tag{20}$$

From these properties we obtain

$$\bar{\psi}(-p,\theta) = -\frac{p}{p-2} a^{-2(p-1)} \bar{\psi}(p-2,\theta), \tag{21}$$

which is required to find the corresponding symmetry for ψ in the physical space. To that end, consider the back-transformation (11) from which follows

$$\begin{aligned}
\partial_r\left[\frac{1}{r^2}\psi(r,\theta)\right] &= \frac{1}{2\pi\,\mathrm{i}}\int_{c-\mathrm{i}\infty}^{c+\mathrm{i}\infty}(-p-2)r^{-p-3}\bar{\psi}(p)\,\mathrm{d}p \\
&\overset{p\to -p}{=} \frac{1}{2\pi\,\mathrm{i}}\int_{-c-\mathrm{i}\infty}^{-c+\mathrm{i}\infty}(p-2)r^{p-3}\bar{\psi}(-p)\,\mathrm{d}p \\
&\overset{\text{using (21)}}{=} \frac{1}{2\pi\,\mathrm{i}}\int_{-c-\mathrm{i}\infty}^{-c+\mathrm{i}\infty}(-p)r^{p-3}a^{-2(p-1)}\bar{\psi}(p-2)\,\mathrm{d}p \\
&= -\frac{1}{r^2}\partial_r\left\{\left(\frac{r}{a}\right)^2\frac{1}{2\pi\,\mathrm{i}}\int_{-c-\mathrm{i}\infty}^{-c+\mathrm{i}\infty}\left(\frac{a^2}{r}\right)^{-(p-2)}\bar{\psi}(p-2)\,\mathrm{d}p\right\} \\
&\overset{q=p-2}{=} -\frac{1}{r^2}\partial_r\left\{\left(\frac{r}{a}\right)^2\frac{1}{2\pi\,\mathrm{i}}\int_{-c-\mathrm{i}\infty-2}^{-c+\mathrm{i}\infty-2}\left(\frac{a^2}{r}\right)^{-q}\bar{\psi}(q)\,\mathrm{d}q\right\}. \qquad (22)
\end{aligned}$$

Setting $c=-1$ we obtain

$$\partial_r\left[\frac{1}{r^2}\psi(r,\theta)\right] = -\frac{1}{r^2}\partial_r\left[\left(\frac{r}{a}\right)^2\psi\left(\frac{a^2}{r},\theta\right)\right]. \qquad (23)$$

This formula enables us to establish the behavior for small $r'=a^2/r\to 0$ once the asymptotic behavior for $r\to\infty$ is known.

The solution of (1, 3) with $c=-1$ reads

$$\begin{aligned}
\psi(r,\theta) &= \frac{1}{2\pi\,\mathrm{i}}\int_{-1-\mathrm{i}\infty}^{-1+\mathrm{i}\infty} r^{-p}\bar{\psi}(p,\theta)\,\mathrm{d}p \\
&= \frac{\omega_0 a^2}{4}\frac{1}{2\pi\,\mathrm{i}}\int_{-1-\mathrm{i}\infty}^{-1+\mathrm{i}\infty}\left(\frac{a}{r}\right)^p\frac{F(\theta,p)}{W(p)(p+1)(p+2)}\,\mathrm{d}p. \qquad (24)
\end{aligned}$$

For $r>a$ the integrand vanishes at infinity and the integral can be closed over the right half plane. The residue theorem yields

$$\psi(r,\theta) = -\frac{\omega_0 a^2}{4}\sum_{\substack{n\\ \Re(p_n)>-1}}\operatorname{Res}\left\{\left(\frac{a}{r}\right)^{p_n}\frac{F(\theta,p_n)}{W(p_n)(p_n+1)(p_n+2)}\right\}, \qquad (25)$$

where p_n denotes the poles of the integrand in (24). Since we can use the residue theorem only for $r>a$ the symmetry relation (23) is necessary to obtain the behavior for $r<a$.

Up to the values of p_n for which $F(\theta,p)$ is zero, the poles of the integrand are determined by the zeros of $W(p)$ for $\Re(p)>-1$. They have been analyzed by Moffatt and Duffy [4], who showed that the zeros are simple except for special intersection points. For simple poles we get

$$\psi(r,\theta) = -\frac{\omega_0 a^2}{4}\sum_{\substack{n\\ \Re(p_n)>-1}}\left(\frac{a}{r}\right)^{p_n}\frac{F(\theta,p_n)}{W'(p_n)(p_n+1)(p_n+2)}, \qquad (26)$$

where

$$W'(p_n) = \sin 2\alpha - 2\alpha \cos[2(p_n+1)\alpha] \neq 0. \tag{27}$$

The leading order term for $r \to \infty$ is due to the residue of the pole having the smallest real part of p. For $\alpha < \alpha_c$, the corresponding pole of $W(p)$ is $p_0 = 0$ [4]. It is real and simple for $\alpha \neq \alpha_c$. However, since $F(\theta, p_0) = 0$ and $F'(\theta, p_0) \neq 0$ with

$$\left.\frac{\partial F(\theta, p)}{\partial p}\right|_{p\to 0} = \sin[2\theta - 2\alpha] + 2\alpha \cos[2\theta - 2\alpha] - \sin[2\theta]$$

$$-2\theta + \sin[2\alpha] + (2\theta - 2\alpha)\cos[2\alpha], \tag{28}$$

the integrand $\sim F(\Theta, p)/W(p)$ has no pole at $p_0 = 0$ in contrast to the hinged plate problem considered in [4]. Thus for $\alpha < \alpha_c$ all poles have $\Re(p_n) > 0$.

5. Asymptotic behavior

We are now in the situation to calculate the solution for small distances from the vertex. Integrating the symmetry relation (23) we get

$$\psi\left(\frac{a^2}{r}, \theta\right) = \frac{\omega_0 a^4}{r^2}\left[\frac{\partial_p F(\theta, 0)}{2W'(0)} + \frac{1}{4}\sum_n \left(\frac{a}{r}\right)^{p_n} \frac{F(\theta, p_n)}{W'(p_n)(p_n+1)p_n}\right], \quad r > a, \tag{29}$$

or, with $r' = a^2/r < a$, and dropping the prime

$$\psi(r, \theta) = \omega_0 r^2\left[\frac{\partial_p F(\theta, 0)}{2W'(0)} + \frac{1}{4}\sum_n \left(\frac{r}{a}\right)^{p_n} \frac{F(\theta, p_n)}{W'(p_n)(p_n+1)p_n}\right], \quad r < a. \tag{30}$$

Since $\Re(p_n) > 1$ for $\alpha < \alpha_c$, the leading order term for $r \to 0$ is produced by $\partial_p F(\theta, 0)/(2W'(0)) = f(\theta)$. It arises here in the course of integration, since the symmetry relation (23) destroys all information on the angular dependence for functions $\sim r^2$. This is a consequence of the symmetry relation being differential rather than algebraic, as for the hinged plate problem. We have thus seen that the similarity solution (4) is in fact the relevant solution for $\alpha < \alpha_c$.

In the case $\alpha > \alpha_c$ the pole with the smallest real part, p_1, is again simple and real and satisfies [4]

$$0 > p_1 \geqslant -\tfrac{1}{2}, \quad \text{for } \alpha_c < \alpha \leqslant \pi. \tag{31}$$

Thus the leading order term in (30) is due to the pole p_1 and we get the asymptotic form of the stream function

$$\psi(r, \theta) \sim \frac{\omega_0}{4} r^2 \left(\frac{r}{a}\right)^{p_1} \frac{F(\theta, p_1)}{W'(p_1)(p_1+1)p_1}, \quad r \to 0. \tag{32}$$

This is obviously not the similarity solution. It is easily seen that the conditions (12) for the existence of the integral (10) are satisfied.

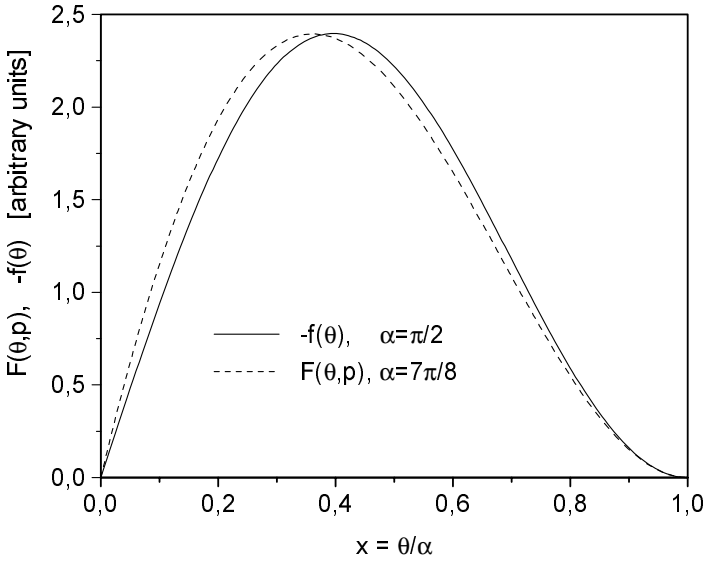

Figure 2. Angular dependence of the asymptotic solution for the stream function, normalized to the maximum value of F. Full line: $\alpha = \pi/2$; dashed line: $\alpha = 7\pi/8$.

To check whether the solution of the Stokes equation for $\alpha > \alpha_c$ is a valid approximation to the respective solution of the Navier-Stokes equation, we compare the order of magnitude of viscous and inertial terms and find that the viscous ones dominate, only if

$$r \ll \left(\frac{\nu}{\omega_0}\right)^{1/(2+p_1)} a^{p_1/(2+p_1)} \stackrel{a\to\infty}{\longrightarrow} 0, \tag{33}$$

where ν is the kinematic viscosity. Thus the radial distance from the vertex within which (32) is a valid approximation to the Navier-Stokes equation shrinks to zero as $a \to \infty$. Therefore, inertia terms cannot be neglected for the infinite wedge problem, no matter how small the length scale is.

We now consider the critical angle $\alpha = \alpha_c$. In [4], the integrand has a double zero at $p_1 = 0$ and $\alpha = \alpha_c$. Here the pole is simple, because $F = W(p)(p+1)(p+2) = \{W(p)(p+1)(p+2)\}' = 0$, $F' \neq 0$, and $\{W(p)(p+1)(p+2)\}'' \neq 0$ for $p = 0$. The residue of the simple pole at $\alpha = \alpha_c$ with $p_1 = 0$ is given by

$$\mathrm{Res}\left\{\left(\frac{a}{r}\right)^{p_1} \frac{F(\theta, p_1)}{W(p_1)(p_1+1)(p_1+2)}\right\} = \frac{1}{W''(0)} \left.\frac{\partial F(\theta, p)}{\partial p}\right|_{p=0}. \tag{34}$$

Using (34) and the symmetry relation (23), we observe that the stream function for small $r \to 0$ takes the asymptotic form

$$\psi(r, \theta) \sim \frac{\omega_0}{2W''(0)} \left.\frac{\partial F(\theta, p)}{\partial p}\right|_{p=0} r^2 \log \frac{r}{a}, \quad r \to 0. \tag{35}$$

6. Discussion

The radial dependence of the asymptotic form of the solutions (4), (35), and (32), namely $\sim r^2$, $\sim r^2 \log r$, and $\sim r^{2+p_1}$, is the same as for the hinged plate problem considered by

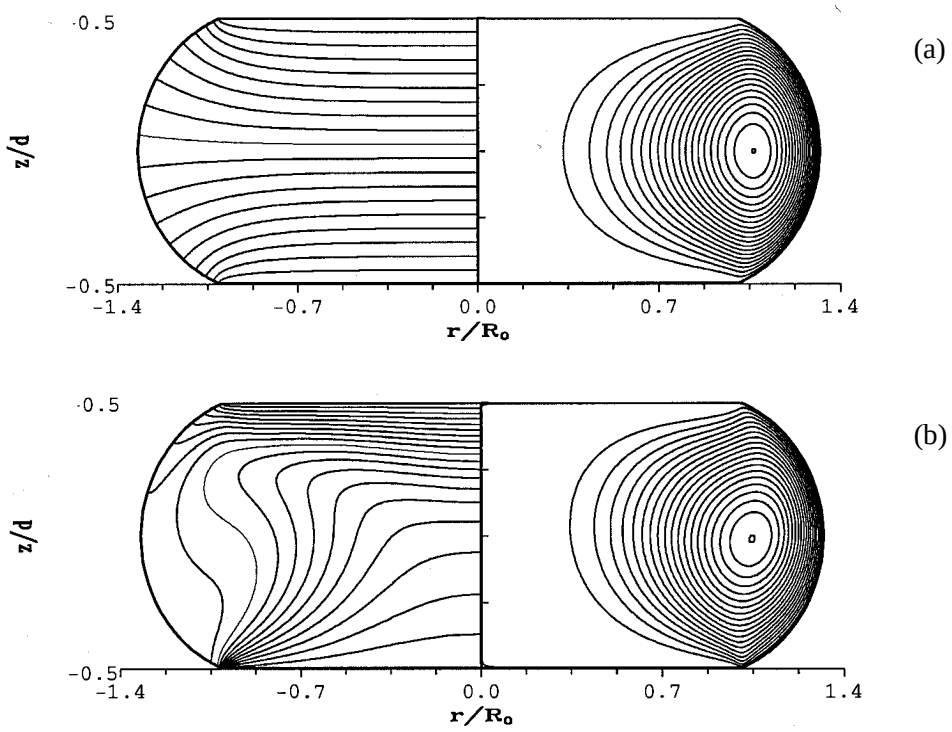

Figure 3. Streamlines (right) and isotherms (left) in a liquid bridge under zero gravity conditions for $\Gamma = 1$, $\mathrm{Pr} = 1$, $\mathrm{Bi} = 0$, $\mathrm{Re} = 10^{-5}$ (a) and $\mathrm{Re} = 2 \times 10^3$ (b). The upper and lower contact angles are $\alpha = 7\pi/8$.

Moffatt and Duffy [4]. As can be seen in Figure 2, the angular dependence of the supercritical solution for $\alpha = 7\pi/8 > \alpha_c$ ($p_1(7\pi/8) = -0{\cdot}3403$) is very similar to that of the subcritical solution for $\alpha = \pi/2 < \alpha_c$.

The present investigation is motivated by the problem of thermocapillary flow near a contact line in an important model for the float-zone crystal-growth process. Hence, we compare the present asymptotic results with numerical calculations of the flow in the so-called half-zone model; see *e.g.* [11]. This model consists of an incompressible liquid held by an asymptotically large mean surface tension between two concentric rigid disks of equal radii but different temperatures. In this limit the interface has a constant curvature and its shape is statically determined. Tangential gradients of the surface temperature induce shear stresses on the free surface that drive the fluid motion. In the absence of gravity the contact angle in barrel-shaped half-zones is larger than $\alpha = \pi/2$ and numerical problems may be encountered if the contact angle exceeds its critical value.

For a comparison we calculated the two-dimensional stationary flow in a half-zone with contact angles $\alpha = \pi/2$ and $\alpha = 7\pi/8$ for Prandtl number $\mathrm{Pr} = 1$, Biot number $\mathrm{Bi} = 0$, aspect ratio $\Gamma = 1$, and Reynolds number $\mathrm{Re} = 10^{-5}$ (see [11] for a definition of the parameters).

The numerical code uses a finite difference method on a 101×101 grid with grid stretching factors of 0·90 and 0·95 which gives a minimum grid spacing near the boundaries of $2{\cdot}9 \times 10^{-4}$ (axially) and $3{\cdot}1 \times 10^{-4}$ (radially), respectively, in units of the disks' radii. Figure 3 shows the streamlines and isotherms in a liquid bridge with $\alpha = 7\pi/8$ for $\mathrm{Re} = 10^{-5}$ (a) and $\mathrm{Re} = 2 \times 10^3$ (b).

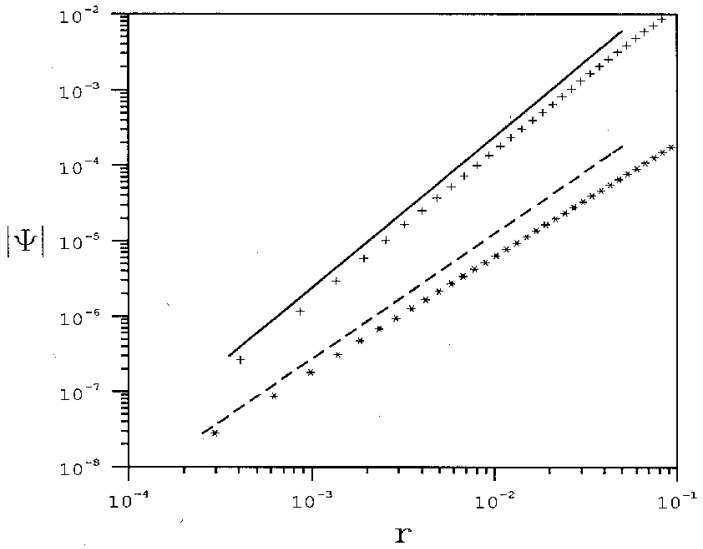

Figure 4. Dependence of the asymptotic solutions (4) and (32) on the distance r from the vertex along the bisection of the wedge angle. Full line: $\alpha = \pi/2$; dashed line: $\alpha = 7\pi/8$. The finite difference numerical data for $\mathrm{Re} = 10^{-5}$ near the cold corner are respresented by plus signs and asterisks.

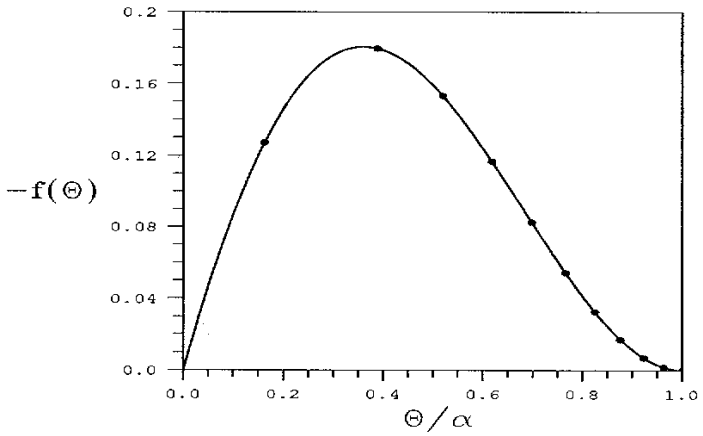

Figure 5. Azimuthal dependence of the stream function for $\alpha = \pi/2$. Full line: Asymptotic solution, dots: Normalized numerical result at $r = 5 \times 10^{-3}$ from the cold corner.

The asymptotic behavior of the flow field near the hot ($z = 0{\cdot}5$) and cold ($z = -0{\cdot}5$) corners is the same. The dependence of the absolute value of the stream function on the distance r from the cold corner contact point in units of the disks radii is shown in Figure 4 along the bisection of the contact angle. For a contact angle of $\alpha = \pi/2$ the slopes computed from successive pairs of numerical data in Figure 4 range from 1·750 to 2·003 (r decreasing). The latter value is in excellent agreement with the theoretical value 2·0. For the large contact angle $\alpha = 7\pi/8$ the agreement is still reasonable. Here the slopes range from 1·489 to 1·580. The latter value is only 5 percent smaller than the theoretical value 1·660. From the curvature of the interpolated numerical data it is expected that the asymptotic regime is even better approached for values of the radial coordinate less than 10^{-3} in this case.

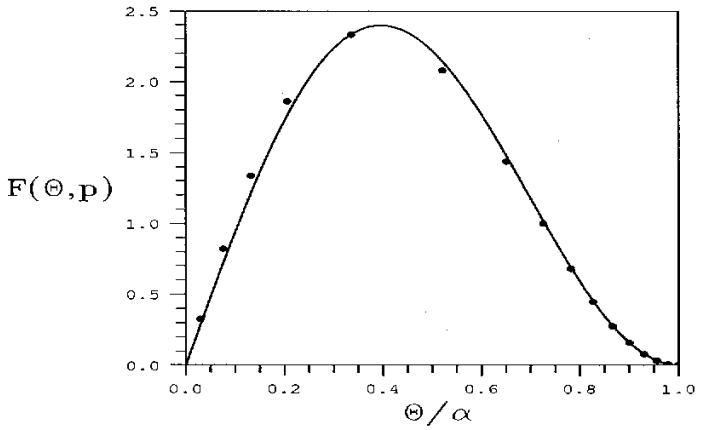

Figure 6. Azimuthal dependence of the stream function for $\alpha = 7\pi/8$. Full line: Asymptotic solution, dots: Normalized numerical result at $r = 5 \times 10^{-3}$ from the cold corner.

Table 1. Comparison at selected angles θ/α between the numerical ($r = 5\times10^{-3}$, Re $= 10^{-5}$) and theoretical data plotted in Figures 5 and 6.

$\alpha = \pi/2$		$\alpha = 7\pi/8$	
θ/α	$(f_{\text{num}} - f)/f$	θ/α	$(F_{\text{num}} - F)/F$
0·162	0·0022	0·076	0·14
0·519	−0·0008	0·206	0·05
0·618	−0·0012	0·521	−0·03
0·766	−0·0015	0·725	−0·02
0·877	−0·0017	0·866	−0·01

The angular dependence of the stream function is shown in Figures 5 and 6 for a distance $r = 5 \times 10^{-3}$ from the cold corner contact line and for a Reynolds number Re $= 10^{-5}$. The deviation from the theoretical θ dependence is quantified in Table 1 for representative values of θ. Since the value of a is not defined in the numerical calculations, the θ dependence can only be compared up to a constant factor. To that end we have normalized the numerical data f_{num} and F_{num} by multiplication with $(f/f_{\text{num}})_{\theta/\alpha=0\cdot389}$ and $(F/F_{\text{num}})_{\theta/\alpha=0\cdot336}$, respectively. The relative deviations range from $-0{\cdot}2$ percent to $0{\cdot}2$ percent for $\alpha = \pi/2$. For the large contact angle the differences are higher (up to 14 percent). This is attributed to the high resolution required, and not provided by the present numerical grid, to fully resolve the asymptotic behavior near the contact line for $\alpha = 7\pi/8$.

The Reynolds numbers in applications are usually much higher than 10^{-5}. For Re $= 2 \times 10^3$ the isotherms become more crowded near the contact lines and the streamlines become 'sucked' into the wedges (cf. Figure 3(b)). Yet, the present analysis likewise applies to this case. Merely, the resolution must be increased to numerically resolve the flow on the small scales on which it takes its asymptotic form.

The foregoing comparison shows the relevance of the present asymptotic solution for the flow in technical applications like, *e.g.* the float-zone process. It provides a means to check the accuracy of numerical calculations near the contact point. Care must be taken to properly resolve the corner flow. An insufficient numerical grid resolution may, otherwise, fake an unphysical flow reversal near the corner. The reason for this effect is probably the sharp increase of the velocity components with the distance from the corner which scale like $\sim r^{1+p_1}$ and increase with infinite slope at $r = 0$.

Acknowledgement

We are very grateful to a referee for careful corrections of an earlier version of this paper. This work was partially supported by DLR under grant number 50WM9443.

References

1. G. I. Taylor, Similarity solutions of hydrodynamic problems. In: *Aeronautics and Astronautics* (Durand Anniversary Volume), Pergamon (1960) pp. 21–28.
2. G. I. Taylor (1962), On scraping viscous fluid from a plane surface. In: G. K. Batchelor (ed.), *The Scientific Papers of Sir Geoffrey Ingram Taylor* **4**. Cambridge University Press (1971) pp. 410–413.
3. H. K. Moffatt, Viscous and resistitive eddies near a sharp corner. *J. Fluid Mech.* 18 (1964) 1–18.
4. H. K. Moffatt and B. R. Duffy, Local similarity solutions and their limitations. *J. Fluid Mech.* 96 (1980) 299–313.
5. D. M. Anderson and S. H. Davis, Two-fluid viscous flow in a corner. *J. Fluid Mech.* 257 (1993) 1–31.
6. D. M. Anderson and S. H. Davis, Fluid flow, heat transfer and solidification near tri-junctions. *J. Crystal Growth* 142 (1994) 245–252.
7. S. Betelú, J. Diez, R. Gratton and L. Thomas, Instantaneous viscous flow in a corner bounded by free surfaces. *Phys. Fluids* 8 (1996) 2269–2274.
8. D. T. L. Hurle (ed), *Handbook of Crystal Growth.* North Holland (1994).
9. T. R. Salamon, D. E. Bornside, R. C. Armstrong and R. A. Brown, The role of surface tension in the dominant balance in the die swell singularity. *Phys. Fluids* 7 (1995) 2328–2344.
10. D. Canright, Thermocapillary flow near a cold wall. *Phys. Fluids* 7 (1994) 1415–1424.
11. V. S. Shevtsova, H. C. Kuhlmann and H. J. Rath, Thermocapillary convection in liquid bridges with a deformed free surface. In: L. Radtke, H. Walter and B. Feuerbacher (eds.), *Materials and Fluids under Low Gravity* vol. 464 of Lecture Notes in Physics. Springer (1996) pp. 323–329.
12. H. K. Moffatt, Viscous eddies near a sharp corner. *Arch. Mech Stosowanej* 16 (1964) 365–372.
13. C. J. Tranter, The use of the Mellin transform in finding the stress distribution in an infinite wedge. *Quart. J. Mech. Appl. Math.* 1 (1948) 125–130.